Published in final edited form as:
J Autoimmun. 2013 February ; 40: 21–27. doi:10.1016/j.jaut.2012.07.008.

Astrocytic autoantibody of neuromyelitis optica (NMO-IgG) binds to aquaporin-4 extracellular loops, monomers, tetramers and high order arrays

Raffaele Iorio[a,b], **James P. Fryer**[a], **Shannon R. Hinson**[a], **Petra Fallier-Becker**[d], **Hartwig Wolburg**[d], **Sean J. Pittock**[a,b], and **Vanda A. Lennon**[a,b,c,*]

[a]Department of Laboratory Medicine and Pathology, Mayo Clinic, 200 First Street S.W., Rochester, Minnesota 55905, USA

[b]Department of Neurology, Mayo Clinic, 200 First Street S.W., Rochester, Minnesota 55905, USA

[c]Department of Immunology, Mayo Clinic, 200 First Street S.W., Rochester, Minnesota 55905, USA

[d]Institute of Pathology and Neuropathology, University of Tübingen, D-72076 Tübingen, Germany

Abstract

The principal central nervous system (CNS) water channel, aquaporin-4 (AQP4), is confined to astrocytic and ependymal membranes and is the target of a pathogenic autoantibody, neuromyelitis optica (NMO)-IgG. This disease-specific autoantibody unifies a spectrum of relapsing CNS autoimmune inflammatory disorders of which NMO exemplifies the classic phenotype. Multiple sclerosis and other immune-mediated demyelinating disorders of the CNS lack a distinctive biomarker. Two AQP4 isoforms, M1 and M23, exist as homotetrameric and heterotetrameric intramembranous particles (IMPs). Orthogonal arrays of predominantly M23 particles (OAPs) are an ultrastructural characteristic of astrocytic membranes. We used high-titered serum from 32 AQP4-IgG-seropositive patients and 85 controls to investigate the nature and molecular location of AQP4 epitopes that bind NMO-IgG, and the influence of supramolecular structure. NMO-IgG bound to denatured AQP4 monomers (68% of cases), to native tetramers and high order arrays (90% of cases), and to AQP4 in live cell membranes (100% of cases). Disease-specific epitopes reside in extracellular loop C more than in loops A or E. IgG binding to intracellular epitopes lacks disease specificity. These observations predict greater disease specificity and sensitivity for tissue-based and cell-based serological assays employing “native” AQP4 than assays employing denatured AQP4 and fragments. NMO-IgG binds most avidly to plasma membrane surface AQP4 epitopes formed by loop interactions within tetramers and by intermolecular interactions within high order structures. The relative abundance and localization of AQP4 high order arrays in distinct CNS regions may explain the variability in clinical phenotype of NMO spectrum disorders.

*Corresponding author: Vanda A. Lennon, M.D., Ph.D., Neuroimmunology Laboratory, Mayo Clinic, 200 First Street S.W., Rochester, MN 55905, USA. Tel: 1-507-284-7514; Fax: 1-507-538-7060; lennon.vanda@mayo.edu.

Disclosures Drs. Iorio, Wolburg and Fallier-Becker and Mr. Fryer report no disclosures.
Drs. Lennon, Pittock and Hinson may accrue revenue for patents regarding aquaporin-4 associated antibodies for diagnosis of neuromyelitis optica and aquaporin-4 autoantibody as a cancer marker.

Keywords

autoimmunity; epitopes; freeze fracture electron microscopy

1. Introduction

Aquaporin-4 (AQP4) is the principal water channel of the central nervous system (CNS) and is the target of an IgG autoantibody that distinguishes the neuromyelitis optica (NMO) spectrum of inflammatory CNS disorders (NMOSD) from multiple sclerosis and other immune-mediated demyelinating CNS disorders [1, 2]. CNS AQP4 is confined to astrocytes and ependymal cells. The two major human AQP4 isoforms, M1 and M23, have identical extracellular residues, but M23 lacks the initial 22 cytoplasmic N-terminal residues of M1 [3, 4]. M1 and M23 exist in the plasma membrane as homotetrameric and heterotetrameric particles. Aggregates of predominantly M23 intramembranous particles (IMPs) form orthogonal arrays (OAPs) [5] that are limited in size by boundary heterotetramerization of M23 with M1 [6]. By using 32 individual NMOSD patient sera containing extremely high levels of NMO-IgG, we comprehensively investigated the nature and molecular location of biologically pertinent B cell epitopes of AQP4, and the influence of supramolecular structure, thus clarifying inconsistencies in earlier reports based on studies of small numbers of sera.

2. Materials and Methods

2.1. Patients

The Mayo Clinic Institutional Review Board approved the study of sera obtained from consenting patients, including 32 with a diagnosis of NMO or NMO spectrum disorder, high serum levels of NMO-IgG by both tissue-based immunofluorescence assay [2] (IFA, titer ≥1:7680) and by immunoprecipitation of solubilized recombinant GFP-AQP4 (IPA, value ≥400 nmol/L) [7], and clinical information including radiological data and timing of immunosuppressant therapies in relation to serum sampling. Twenty-three of the 32 patients fulfilled 2006 diagnostic criteria for NMO [8] and 9 had a partial form of NMO (i.e., NMO-IgG seropositivity with relapsing longitudinally extensive transverse myelitis [6 patients] or relapsing optic neuritis [3 patients]). Table 1 summarizes demographic and clinical data of the study subjects.

Control subjects were matched for age and sex: 32 healthy subjects, 18 patients with multiple sclerosis (fulfilling 2010 McDonald diagnostic criteria [9]) and 35 patients with idiopathic or paraneoplastic autoimmune neurological disorders accompanied by the following neural-specific IgGs: muscle acetylcholine receptor (AChR), 5; collapsin response-mediator protein-5 (CRMP-5), 7; glutamic acid decarboxylase (GAD65), 3; anti-neuronal nuclear antibody (ANNA) type-1, 4, or ANNA-2, 1; Purkinje cell cytoplasmic antibody, type-1 (PCA-1), 7; amphiphysin, 5 and voltage-gated potassium channel (VGKC)-complex, 3.

2.2. DNA constructs, cell culture and transfection

cDNAs corresponding to AQP4-M1 and AQP4-M23 (non-tagged) were cloned into pcDNA3.1 expression vectors [10] and the vector integrity and DNA sequences were verified. Stable cell lines were established by transfecting human embryonic kidney (HEK293) cells with plasmid DNA using Fugene 6 (Promega Corp., Madison, WI). Clones emerging under selective pressure (Hygromycin 200 μg/mL) were tested for AQP4 protein

(western blot) and surface expression (indirect immunofluorescence). Those expressing M1 or M23 protein at similar levels were selected for expansion.

2.3. Synthetic peptides and fusion proteins

Synthetic peptides (Fig. 1A) corresponded to extracellular segments of rat AQP4 (loops A [54–69], C [137–157] and E [207–231]) and intracellular segments of human AQP4 (N-terminus [1–22], loop B [94–114] and C-terminus [253–272]). GST fusion proteins (Fig. 1B) corresponded to human AQP4 extracellular loops A [56–71], C [135–159] and E [205–231]. Each was purified by adsorption to glutathione-Sepharose 0.2 mM EDTA, 1 mM PMSF, and the size and purity was verified by SDS-PAGE. Protein concentration was determined by Bradford Assay.

2.4. Freeze-fracture electron microscopy

Monolayer cell cultures were fixed 2 hr at 22 °C with 2.5% glutaraldehyde in 0.1 M cacodylate buffer (pH 7.4), cryoprotected in 30% glycerol and quick-frozen in nitrogen-slush (−210°C). The specimens were fractured at 5×10^{-6} mbar and −150°C (BAF400D; Balzers, Liechtenstein). Fracture faces were shadowed with platinum/carbon (2.5 nm, 45°) for contrast and carb on (25 nm, 90°) for stabilization of the replica. After removing the cell material 12% sodium hypochlorite, the replicas. were cleaned several times in double-distilled water, mounted on Pioloform-coated copper grids and viewed using a Zeiss EM10 electron microscope (Oberkochen, Germany).

2.5. Indirect immunofluorescence

Sera were analyzed at 4°C for IgG reactive with the AQP4 extracellular domain in a live cell binding assay [1] using HEK293 cells transfected with M1 or M23, or nontransfected (control). After blocking for 30 min with 10% goat serum in phosphate buffered saline (PBS), serum was applied at 1:10 dilution. After 1 hr the cells were washed in chilled PBS and exposed to fluorescein-conjugated goat IgG specific for human IgG (BD Biosciences, San Jose, CA). After 30 min, they were washed in PBS, fixed in 4% paraformaldehyde (PFA) and mounted in ProLong Gold antifade mounting medium (Molecular Probes, Life Technologies Corp., Grand Island, NY). For intracellular staining, cells were rinsed in PBS, fixed for 15 min in cold 95% ethanol/5% acetic acid, washed in PBS and permeabilized for 3 min in 0.1% triton-X-100. After blocking 30 min in 10% goat serum, cells were exposed 16 hr at 4°C to rabbit IgG raised against rat AQP4 residues 249–323 (Sigma-Aldrich Co., LLC, St. Louis, MO; 1:500 dilution), washed, then exposed 1 hr to TRITC-conjugated anti-rabbit-IgG (SouthernBiotech, Birmingham, AL).

2.6. Immunochemical analyses

2.6.1. Blue native-PAGE (BN-PAGE)—HEK293 cells were lysed at 4°C in NativePAGE sampl e buffer (Invitrogen) containing 0.5% dodecyl-B-D-maltoside (DDM/protein ratio 4:1 g/g). Supernatant protein concentration of clarified lysates (20,000 g, 10 min, 4°C) was determined by BCA assay. Equal amounts (5 μg) were mixed with 0.5% G-250 (detergent: G-250 ratio, 4:1), loaded in Bis-Tris gel (3–12%) and electrophoresed using NativePAGE running buffers (by manufacturer instructions). After soaking the gels in 0.1% SDS for 10 min, proteins were transferred to PVDF membrane and fixed in 8% acetic acid. Coomassie G250 was removed by twice soaking for 2 hr in 0.2% Tween-20, 10 mM imidazole/HCl (pH 7.0).

2.6.2. SDS-PAGE—Membranes prepared from transfected HEK293 cells, or Ni-affinity-purified fusion proteins, were mixed 1:1 with 2× SDS Laemmli buffer, electrophoresed in 10% polyacrylamide and transferred to PVDF membrane. After washing twice with TTBS,

PVDF membranes were stained for 1 min with 0.1% Coomassie blue 1:1 in methanol/water, or with 0.1% Ponceau S in 5% acetic acid. Blots were blocked for 16 hr in buffer containing 20 mM Tris, pH 7.6, 137 mM sodium chloride, 0.1% Tween-20 (TBST) containing 10% nonfat dry milk, and probed with sera from patients with NMOSD or other neurological disorders, or healthy subjects' sera (diluted from 1:50 to 1:500), or with control polyclonal rabbit IgG specific for AQP4 C-terminus (Sigma-Aldrich; diluted 1:2000). After washing in TBST, bound IgG was detected autoradiographically by enhanced chemiluminescence (Thermo Fisher Scientific, Inc., Rockford, IL) using horseradish peroxidase-conjugated goat IgG specific for human IgG or rabbit IgG (SouthernBiotech).

2.6.3. ELISA—Serum was diluted in doubling steps (from 1:100 to immunoreactivity endpoint) in PBS containing goat serum (10%) and Tween-20 (0.05%), and added to 96-well plates (Immulon 2 HB) coated with peptide (0.75 μM, in 100 μL of 0.01M phosphate buffer, pH 7.4). After holding at 37°C (2 hr) then at 4°C (16 hr), plates were washed 3 times with PBS/0.05% Tween-20. Bound IgG was detected using alkaline phosphataseconjugated goat IgG specific for human IgG and p-NO2-phenyl phosphate substrate. Values considered positive exceeded 150% of the mean OD_{405} value yielded by 10 normal control sera at each dilution.

2.7. Statistical analyses

Comparisons between different groups of sera were performed using Fisher's exact test.

3. Results

3.1. AQP4 M23 forms orthogonal array-like assemblies of particles in stably transfected HEK293 cells

Fluorescence microscopy revealed a diffuse distribution of AQP4 immunoreactivity at the surface of M1 cells (Fig. 2A). Plasma membranes of M23 cells had a more punctate distribution of immunoreactivity (Fig. 2B). Freeze-fracture electron microscopy revealed numerous IMPs on the P-face of M1 cell membranes, but no OAP-like structures (Fig. 2C). By contrast, the scattered IMP aggregates on the P-face of M23 cell membranes (Fig. 2D), resembling lattices of orthogonal array particles, were interpreted to correspond to the punctate distribution of AQP4 immunoreactivity in Fig. 2B [11].

3.2. NMO-IgG binds to the extracellular domain of both M1 and M23

Extracellular domain amino acid sequences are identical in both AQP4 isoforms. Earlier investigators have reported that NMO-IgG binds selectively to the M1 isoform [12] or the M23 isoform [13]. Our live cell binding assays revealed that IgG in sera of all NMOSD patients bound to surface epitopes in both M1 and M23 cells, confirming the report of Crane et al. [14]. The immunoreactivity of M23 cells was generally more intense than that of M1 cells reflecting the greater membrane abundance of M23 aggregates (Figs. 2A and 3A). No healthy subject serum or disease control patient serum bound to M1 or M23 cells (Fig. 3A). Rabbit IgG specific for cytoplasmic AQP4 epitopes did not bind to live cells (Fig. 3A). No immunoreactive translational product of M23 size was detectable in M1 cell lysates by SDS-PAGE Western blot analysis with AQP4-specific rabbit IgG (Fig. 3B).

3.3. Binding to AQP4 M1 and M23 monomers, tetramers and high order arrays

To investigate NMO-IgG binding to epitopes intrinsic to M1 and M23 tetramers, and to epitopes dependent on higher order structures formed by tetramer intermolecular interactions, we employed BN-PAGE to separate AQP4 tetramers and high order arrays solubilized in “native form” from cell lines transfected with M1 or M23 [15]. Western blot

analysis revealed that IgG in 29 of 32 individual NMOSD patients' sera (90%) bound to both M1 and M23 tetramers and to M1 and M23 IMPs and high order arrays. Fig. 3B illustrates representative positive sera.

To investigate the binding of NMO-IgG to denatured epitopes, we resolved solubilized M1 and M23 monomers by SDS-PAGE. Western blot analysis revealed that IgG in 21 of 32 NMOSD patients' sera (68%) bound to both M1 and M23 monomers (Fig. 3B). This indicated binding to continuous epitopes of AQP4. No IgG in any healthy subject or disease control serum bound to denatured or native full-length AQP4 proteins.

3.4. Binding to isolated AQP4 extracellular loop segments

Because IgG in 100% of the evaluated NMOSD sera bound to live M1 and M23 cells, and IgG in 68% of those sera also bound to denatured M1 and M23 proteins, with absolute disease specificity in both instances, we investigated by ELISA the binding of NMO-IgG to synthetic peptides containing AQP4 loop A, C and E sequences (potentially continuous extracellular epitopes; Figs. 1, 4A, C). We further investigated the reproducibility of all observed binding by re-testing sera that yielded positive results for potential western blot reactivity with GST fusion proteins containing the same linear sequences (Fig. 4B, C). IgG in 15 of 32 NMOSD patients' sera (47%) bound to at least one isolated extracellular loop polypeptide (data are summarized in Table 2). In 9 cases (28%) IgG bound to more than one isolated peptide; in 4 cases (12%) IgG bound to 2 extracellular loop peptides and in 5 cases (16%) IgG bound to all 3 loop peptides (Table 2; Fig. 4).

IgG binding to the loop C polypeptide was restricted to patients whose diagnosis was NMO or NMOSD. No healthy subject IgG bound to any peptide or fusion protein, but IgG in 4 of 53 disease control subjects' sera (8%) bound singly to a loop A or loop E peptide (Table 2). Diagnoses in those 4 patients were multiple sclerosis (1), araneoplastic autoimmune (PCA-1/anti-Yo) cerebellar degeneration (2) and voltage-gated potassium channel-complex encephalitis (1). Because no control serum bound to the intact AQP4 protein in native or denatured form, we attributed the binding of control subjects' sera to loops A and E to low affinity IgG-peptide interactions. The data imply lack of disease specificity except for loop C. Reactivity with more than 1 loop peptide was restricted to NMO/NMOSD diagnosis.

3.5. NMO-IgG binding to AQP4 intracellular epitopes

Kampylafka et al. reported that NMO-IgG was more reactive with 3 intracellular segments of AQP4 than with the extracellular loop C segment [16]. We therefore tested our study patients' sera by ELISA for reactivity with peptides representative of those 3 segments. IgG in 9 NMOSD patients' sera (28%) bound to the N-terminus, 12 (37.5%) bound to the loop B peptide and 7 (22%) bound to the C-terminus peptide (Fig. 5). However, disease specificity was excluded by the binding of IgG in 7 healthy subjects' sera and in 35 disease control sera to at least one of these peptides.

4. Discussion

IgG-AQP4 interaction on live cell surfaces initiates multiple molecular sequelae that plausibly account for the diversity of NMO neuropathology (edema, inflammation, demyelination and necrosis), and some of these outcomes are isoform specific [10, 17, 18]. This study illustrates the polyclonality of NMO-IgG, its specificities for multiple conformations of AQP4, and tertiary AQP4 structures as a determinant of binding avidity. Both M1 and M23 tetramers contain disease-specific epitopes that are represented in extracellular loop C more than in loops A and E. The relative abundance and localization of AQP4 high order arrays in different CNS regions, and at different stages of CNS maturity

may influence the phenotypic variability observed in adult and pediatric NMO spectrum disorders.

Earlier studies addressing the antigenic determinants of human AQP4 to which NMO-IgG binds used small numbers of serum specimens, and yielded conflicting data concerning the selectivity of NMO-IgG for M1 or M23 isoforms [6, 12, 13]. Our study of serum from 32 patients with NMO spectrum disorders revealed that all contained IgG that bound, with absolute disease specificity, to extracellular epitopes of both M1 and M23 in live cells. Next we evaluated the specificity of NMO-IgG binding to AQP4 at the molecular and supramolecular levels and in native and denatured forms. IgG in most patients' sera bound to solubilized AQP4 in native tetrameric form and in high order arrays. From a study of just 4 patients' sera, Nicchia et al. concluded that M23 high order arrays are the exclusive target of NMO-IgG [13]. However, numerous independent laboratories have demonstrated unequivocal binding of NMO-IgG to cells expressing the M1 isoform of AQP4 [19–21]. Clinical assays for AQP4 autoantibodies commonly use a recombinant M1 AQP4 protein as antigen [1, 19]. Importantly, our western blot data refute the leaky-scanning hypothesis proposed by Rossi et al. to explain reports of NMO-IgG binding to recombinantly expressed M1 protein [22]; we found no evidence for an M23 translational product arising in cells transfected with cDNA encoding M1. Our findings overall are compatible with the results of Crane et al. whose kinetic comparison of the binding of NMO-IgG to human AQP4 M1 and M23 isoforms demonstrated that NMO-IgG binds to both isoforms in live cell membranes, but more avidly to M23 [14].

Surprisingly, NMO-IgG in more than two-thirds of our study cases also bound to denatured monomeric AQP4 with absolute disease specificity. Previous western blot studies employing lysates of rat cerebrum, cerebellum and kidney tissues have implied lack of NMO-IgG reactivity with denatured AQP4 epitopes [13, 23]. Our unambiguous demonstration of NMO-IgG reactivity with denatured AQP4 was enabled by extracting proteins from membrane fragments of cells transfected with M1 or M23 and by use of high-titered sera. This finding accords with a report that NMO-IgG reacted with continuous epitopes of AQP4 immunopurified from mouse kidney lysates [12]. However, our results do not support the authors' conclusion that disease-pertinent AQP4 epitopes are largely confined to the M1 isoform of AQP4, which implies epitope confinement to the M1-unique cytoplasmic N-terminus [3]). Our study's finding that IgG binding to AQP4 N-terminal residues lacks disease specificity contradicts this conclusion, and contradicts other reports of disease-specific binding of NMO-IgG to linearized intracellular epitopes of AQP4 [16].

X-ray crystallography studies predict 3 extracellular loops connecting the transmembrane helices of AQP4 [24]. Our study revealed that in 47% of cases NMO-IgG bound to one or more peptide fragments representing these individual loops of AQP4. The relatively low frequency of IgG reactivity with the peptides reflects limited flexibility of immobilized peptides and lack of potential post-translational modifications and tertiary structures contributing to antigenicity. Binding to loop C (31%) was 100% disease-specific. Although binding to loop A and E peptides had imperfect disease specificity, binding of disease control sera was infrequent (<3.8%) and no control serum bound to more than one peptide (Table 2). Loop A and E peptides contain several charged residues suitable for the H-bonding and salt bridge interactions that determine antibody binding affinity [25].

Loop C, the longest extracellular segment of AQP4, is predicted to be highly flexible [24, 25], a property anticipated in this peptide. Pisani et al. concluded from an investigation of NMO-IgG binding to engineered mutants of human AQP4, that the tip of loop C (AQP4 residues 146–150) contains a major discontinuous epitope that is recognized only in high order array structures [26].

In sum, our observations predict greater disease specificity for tissue-based and cell-based serological assays employing native AQP4 than assays employing denatured AQP4 or AQP4 fragments. The findings are consistent with NMO-IgG being polyclonal with respect to epitope specificity, and binding most avidly to AQP4 epitopes formed by loop interactions in the tetrameric membrane-bound AQP4 protein and by intermolecular interactions within higher order structures.

Acknowledgments

We thank Thomas Kryzer and Evelyn Posthumus for technical assistance.

Dr. Pittock has received research support from Alexion Pharmaceuticals, Inc. and the NIH (RO1 NS065829-01).

Funding This work was supported by grants from the Guthy-Jackson Charitable Foundation (VAL and SJP), the National Institute of Neurological Disorders and Stroke (R01-NS065829, SJP) and the Deutsche Krebshilfe-Mildred Scheel-Stiftung (109219, HW).

References

[1]. Lennon VA, Kryzer TJ, Pittock SJ, Verkman AS, Hinson SR. IgG marker of optic-spinal multiple sclerosis binds to the aquaporin-4 water channel. J Exp Med. 2005; 202:473–7. [PubMed: 16087714]

[2]. Lennon VA, Wingerchuk DM, Kryzer TJ, Pittock SJ, Lucchinetti CF, Fujihara K, et al. A serum autoantibody marker of neuromyelitis optica: distinction from multiple sclerosis. Lancet. 2004; 364:2106–12. [PubMed: 15589308]

[3]. Hasegawa H, Ma T, Skach W, Matthay MA, Verkman AS. Molecular cloning of a mercurial-insensitive water channel expressed in selected water-transporting tissues. J Biol Chem. 1994; 269:5497–500. [PubMed: 7509789]

[4]. Jung JS, Bhat RV, Preston GM, Guggino WB, Baraban JM, Agre P. Molecular characterization of an aquaporin cDNA from brain: candidate osmoreceptor and regulator of water balance. Proc Natl Acad Sci U S A. 1994; 91:13052–6. [PubMed: 7528931]

[5]. Furman CS, Gorelick-Feldman DA, Davidson KG, Yasumura T, Neely JD, Agre P, et al. Aquaporin-4 square array assembly: opposing actions of M1 and M23 isoforms. Proc Natl Acad Sci U S A. 2003; 100:13609–14. [PubMed: 14597700]

[6]. Crane JM, Bennett JL, Verkman AS. Live cell analysis of aquaporin-4 m1/m23 interactions and regulated orthogonal array assembly in glial cells. J Biol Chem. 2009; 284:35850–60. [PubMed: 19843522]

[7]. McKeon A, Fryer JP, Apiwattanakul M, Lennon VA, Hinson SR, Kryzer TJ, et al. Diagnosis of neuromyelitis spectrum disorders: comparative sensitivities and specificities of immunohistochemical and immunoprecipitation assays. Arch Neurol. 2009; 66:1134–8. [PubMed: 19752303]

[8]. Wingerchuk DM, Lennon VA, Pittock SJ, Lucchinetti CF, Weinshenker BG. Revised diagnostic criteria for neuromyelitis optica. Neurology. 2006; 66:1485–9. [PubMed: 16717206]

[9]. Polman CH, Reingold SC, Banwell B, Clanet M, Cohen JA, Filippi M, et al. Diagnostic criteria for multiple sclerosis: 2010 revisions to the McDonald criteria. Ann Neurol. 2011; 69:292–302. [PubMed: 21387374]

[10]. Hinson SR, Romero MF, Popescu BF, Lucchinetti CF, Fryer JP, Wolburg H, et al. Molecular outcomes of neuromyelitis optica (NMO)-IgG binding to aquaporin-4 in astrocytes. Proc Natl Acad Sci USA. 2012; 109:1245–50. [PubMed: 22128336]

[11]. Wolburg H, Wolburg-Buchholz K, Fallier-Becker P, Noell S, Mack AF. Structure and functions of aquaporin-4-based orthogonal arrays of particles. Int Rev Cell Mol Biol. 2011; 287:1–41. [PubMed: 21414585]

[12]. Marnetto F, Hellias B, Granieri L, Frau J, Patanella AK, Nytrova P, et al. Western blot analysis for the detection of serum antibodies recognizing linear Aquaporin-4 epitopes in patients with Neuromyelitis Optica. J Neuroimmunol. 2009; 217:74–9. [PubMed: 19850359]

[13]. Nicchia GP, Mastrototaro M, Rossi A, Pisani F, Tortorella C, Ruggieri M, et al. Aquaporin-4 orthogonal arrays of particles are the target for neuromyelitis optica autoantibodies. Glia. 2009; 57:1363–73. [PubMed: 19229993]

[14]. Crane JM, Lam C, Rossi A, Gupta T, Bennett JL, Verkman AS. Binding affinity and specificity of neuromyelitis optica autoantibodies to aquaporin-4 M1/M23 isoforms and orthogonal arrays. J Biol Chem. 2011; 286:16516–24. [PubMed: 21454592]

[15]. Sorbo JG, Moe SE, Ottersen OP, Holen T. The molecular composition of square arrays. Biochemistry. 2008; 47:2631–7. [PubMed: 18247481]

[16]. Kampylafka EI, Routsias JG, Alexopoulos H, Dalakas MC, Moutsopoulos HM, Tzioufas AG. Fine specificity of antibodies against AQP4: epitope mapping reveals intracellular epitopes. J Autoimmun. 2011; 36:221–7. [PubMed: 21333492]

[17]. Hinson SR, Pittock SJ, Lucchinetti CF, Roemer SF, Fryer JP, Kryzer TJ, et al. Pathogenic potential of IgG binding to water channel extracellular domain in neuromyelitis optica. Neurology. 2007; 69:2221–31. [PubMed: 17928579]

[18]. Hinson SR, Roemer SF, Lucchinetti CF, Fryer JP, Kryzer TJ, Chamberlain JL, et al. Aquaporin-4-binding autoantibodies in patients with neuromyelitis optica impair glutamate transport by down-regulating EAAT2. J Exp Med. 2008; 205:2473–81. [PubMed: 18838545]

[19]. Waters PJ, McKeon A, Leite MI, Rajasekharan S, Lennon VA, Villalobos A, et al. Serologic diagnosis of NMO: a multicenter comparison of aquaporin-4-IgG assays. Neurology. 2012; 78:665–71. discussion 9. [PubMed: 22302543]

[20]. Bennett JL, Lam C, Kalluri SR, Saikali P, Bautista K, Dupree C, et al. Intrathecal pathogenic anti-aquaporin-4 antibodies in early neuromyelitis optica. Ann Neurol. 2009; 66:617–29. [PubMed: 19938104]

[21]. Mader S, Lutterotti A, Di Pauli F, Kuenz B, Schanda K, Aboul-Enein F, et al. Patterns of antibody binding to aquaporin-4 isoforms in neuromyelitis optica. PLoS One. 2010; 5:e10455. [PubMed: 20463974]

[22]. Rossi A, Pisani F, Nicchia GP, Svelto M, Frigeri A. Evidences for a leaky scanning mechanism for the synthesis of the shorter M23 protein isoform of aquaporin-4: implication in orthogonal array formation and neuromyelitis optica antibody interaction. J Biol Chem. 2010; 285:4562–9. [PubMed: 20007705]

[23]. Tani T, Sakimura K, Tsujita M, Nakada T, Tanaka M, Nishizawa M, et al. Identification of binding sites for anti-aquaporin 4 antibodies in patients with neuromyelitis optica. J Neuroimmunol. 2009; 211:110–3. [PubMed: 19410301]

[24]. Hiroaki Y, Tani K, Kamegawa A, Gyobu N, Nishikawa K, Suzuki H, et al. Implications of the aquaporin-4 structure on array formation and cell adhesion. J Mol Biol. 2006; 355:628–39. [PubMed: 16325200]

[25]. Ho JD, Yeh R, Sandstrom A, Chorny I, Harries WE, Robbins RA, et al. Crystal structure of human aquaporin 4 at 1.8 A and its mechanism of conductance. Proc Natl Acad Sci U S A. 2009; 106:7437–42. [PubMed: 19383790]

[26]. Pisani F, Mastrototaro M, Rossi A, Nicchia GP, Tortorella C, Ruggieri M, et al. Identification of two major conformational aquaporin-4 epitopes for neuromyelitis optica autoantibody binding. J Biol Chem. 2011; 286:9216–24. [PubMed: 21212277]

Highlights

- Neuromyelitis optica (NMO) IgG is disease-specific autoantibody and polyclonal in epitope specificities
- Major epitopes reside in the aquaporin-4 water channel extracellular domain, predominantly loop C
- Tertiary structures determining NMO-IgG binding avidity include loop interactions within tetramers and intermolecular interactions within high order structures

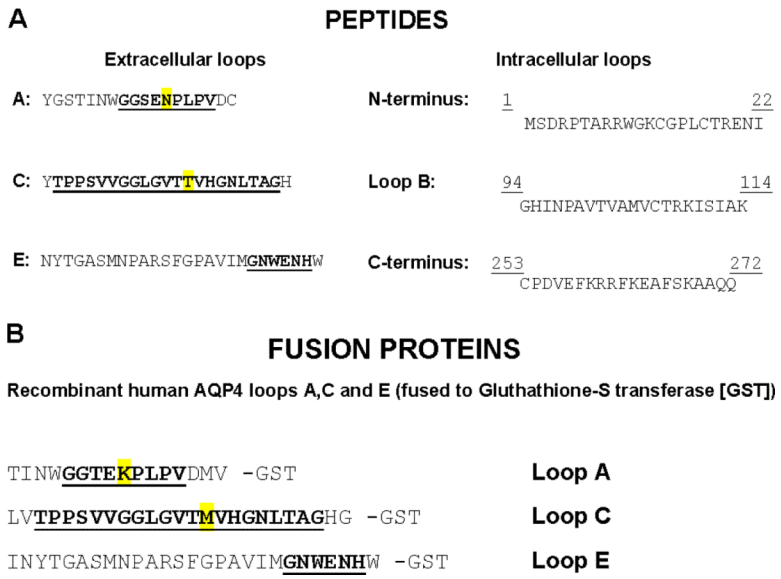

Figure 1.

A) Synthetic peptides corresponding to extracellular loops A (54–69), C (137–157) and E (207–231) of rat AQP4, and human AQP4 intracellular segments: N-terminal residues (1–22), loop B (94–114) and C-terminal residues (253–272). Extracellular loops A and C differ in rat and human AQP4 at 1 residue (highlighted in yellow); loop E is identical in rat and human AQP4. B) GST fusion proteins corresponding to extracellular loops A, C and E of human AQP4. Putative extracellular residues are bold and underlined.

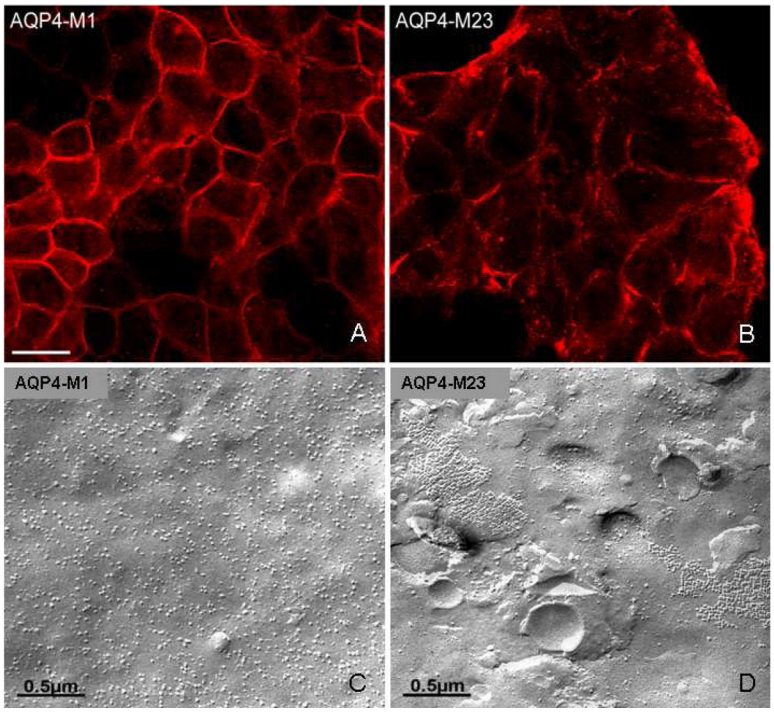

Figure 2.

A, B) Distribution of AQP4 immunoreactivity in plasma membranes of HEK293 cells transfected singly with plasmids encoding either M1 or M23 isoforms (imaged by confocal microscopy). M1 and M23 are identical in extracellular domain sequence. Their common C-terminal cytoplasmic segments were detected by a peptide-specific rabbit IgG (after fixation and permeabilization). AQP4 distribution is “continuous” in M1 membranes (note linear appearance at margins), but is discontinuous in M23 membranes. C, D) Freeze-fracture electron microscopic images of M1 and M23 membranes reveal singlet intramembranous particles in M1 cells. By contrast, most particles in M23 membranes appear as large lattices of orthogonal array-like assemblies. Note absence of lattices in M1 cells.

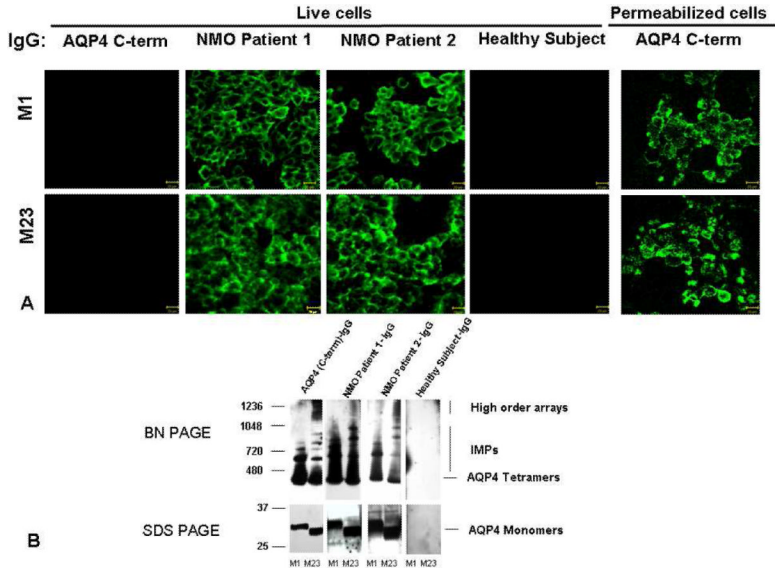

Figure 3.

A) Indirect immunofluorescence reveals disease-specific IgG binding to the extracellular domain of AQP4 in live HEK293 cells transfected with M1 or M23, as illustrated by sera of 2 NMOSD patients. Healthy (and disease control) serum IgG does not bind. By contrast, rabbit IgG specific for cytoplasmic AQP4 epitopes (C-terminal residues 249–323) binds only to permeabilized cells. B) Western blot analysis of M1 and M23 cell lysate proteins separated in “native” form by BN-PAGE and in denatured form by SDS PAGE. IgG in serum of 2 illustrative NMOSD patients binds to AQP4 tetramers and intramembranous particles (M1 and M23) and to high order arrays (M23), and to monomers of each AQP4 isoform. IgG in a representative healthy control human serum does not bind to any AQP4 protein. The control rabbit IgG is specific for AQP4 C-terminal residues. Note: M1 cells lack evidence of an M23 polypeptide product.

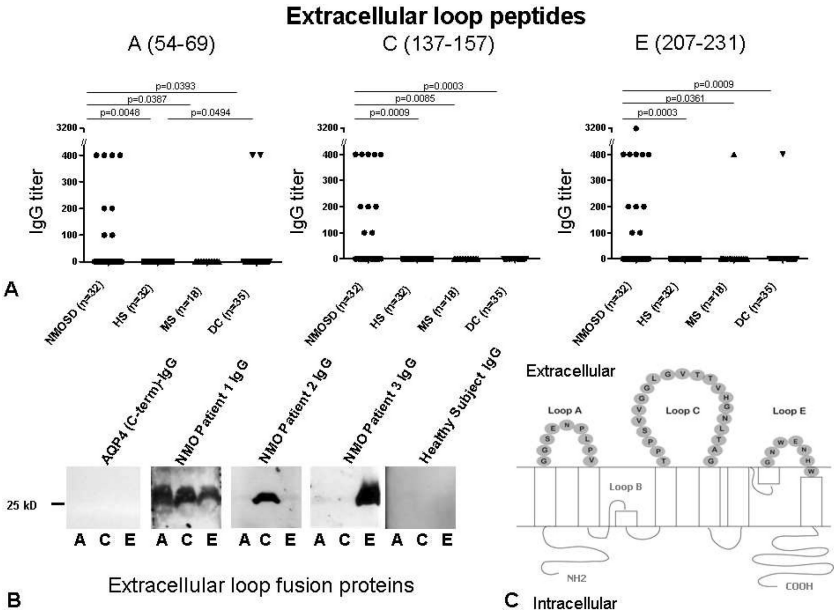

Figure 4.

A) Frequency of IgG reactive with peptides corresponding to AQP4 extracellular loops (detected by ELISA). The statistical significance of comparisons among groups is presented (cutoff for significance p=<0.05). B) Illustrative results of western blot analyses using human AQP4 extracellular loop GST fusion proteins. C) Schematic representation of human AQP4 residues constituting extracellular loops A, C and E.

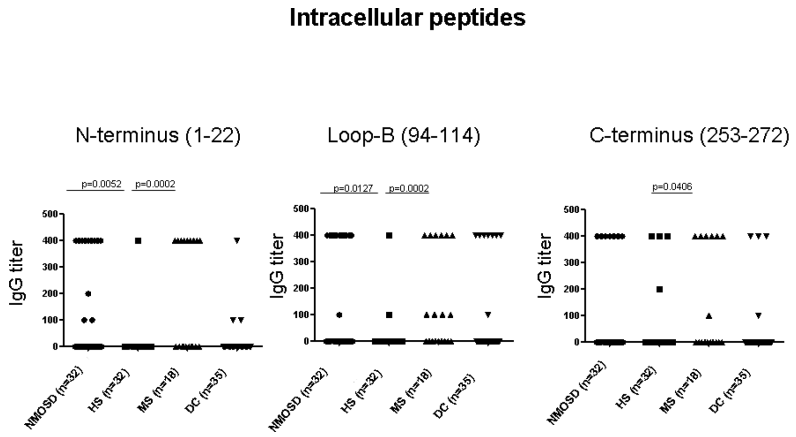

Figure 5.

Frequency of IgG reactive with peptides corresponding to AQP4 intracellular loops (detected by ELISA). The significance of comparisons among groups ($p=<0.05$) was determined by Fisher's Exact test.

Table 1

Clinical and demographic data for study subjects

	NMOSD[a] (n=32)	Healthy adult subjects (n=32)	Multiple sclerosis (n=18)	Miscellaneous autoimmune neurological disorders (n=35)
Mean age (yrs)	47 (15–81)	-	41 (23–70)	46 (19–75)
Female	26 (81%)	-	14 (77%)	26 (74%)
Clinical status	attack, 16 remission, 16	-	attack, 9 remission, 9	-

[a]NMOSD: neuromyelitis optica spectrum disorders (NMO and partial forms: i.e., recurrent optic neuritis or recurrent longitudinal transverse myelitis with NMO-IgG seropositivity).

Table 2

IgG detected by enzyme-linked immunosorbent and western blot assays[a]

AQP4 extracellular loop peptides	NMOSD[b] (n=32)	Healthy subjects (n=32)	Multiple sclerosis (n=18)	Miscellaneous autoimmune neurological disorders (n=35)
Loop A	8 (25%)	0 (p=0.0048)	0 (p=0.0387)	2 (p=0.0393)
Loop C	10 ***(31%)***	0 (p=0.0009)	0 (p=0.0085)	0 (p=0.0003)
Loop E	11 (34%)	0 (p=0.0003)	1 (p=0.0361)	1 (p=0.0009)
Loop A, C or E	15 (47%)	0 (p=0.0001)	1 (p=0.0036)	3 (p=0.0007)
Loops A and C and E	5 ***(16%)***	0 (ns)	0 (ns)	0 (p=0.0248)
Loops A and E	2 ***(6%)***	0 (ns)	0 (ns)	0 (ns)
Loops C and E	2 ***(6%)***	0 (ns)	0 (ns)	0 (ns)
Loops A and C	0	0	0	0

[a] AII sera reactive with loop peptides yielded concordant results in ELISA and western blot analyses.

[b] NMOSD: neuromyelitis optica spectrum disorders (NMO and partial forms); ns: not significant.